DTU Library

Confinement of Rh nanoparticles in triphenylphosphine oxide-functionalized core-crosslinked micelles for aqueous biphasic hydrogenation catalysis

Abou-Fayssal, Chantal J.; Fliedel, Christophe; Poli, Rinaldo; Riisager, Anders; Philippot, Karine; Manoury, Eric

[Link back to DTU Orbit](#)

Contents lists available at ScienceDirect

Materials Today Chemistry

Confinement of Rh nanoparticles in triphenylphosphine oxide-functionalized core-crosslinked micelles for aqueous biphasic hydrogenation catalysis

Chantal J. Abou-Fayssal [a,b], Christophe Fliedel [b], Rinaldo Poli [b,c,**], Anders Riisager [a,*], Karine Philippot [b,***], Eric Manoury [b,****]

[a] Centre for Catalysis and Sustainable Chemistry, Department of Chemistry, Technical University of Denmark, Kemitorvet, Building 207, 2800, Kgs. Lyngby, Denmark
[b] CNRS, LCC (Laboratoire de Chimie de Coordination), Université de Toulouse, UPS, INPT, 205 Route de Narbonne, BP 44099, F-31077, Toulouse, Cedex 4, France
[c] Institut Universitaire de France, 1, Rue Descartes, 75231, Paris, Cedex 05, France

ARTICLE INFO

ABSTRACT

The introduction of phosphine oxide as anchoring groups in the hydrophobic core of amphiphilic star-block copolymers leads to greatly improved confinement of rhodium nanoparticles (RhNPs) inside the nanoreactors with a benefit in aqueous biphasic catalysis. The copolymers are specially designed core-crosslinked micelles (CCMs) forming a stable latex by reversible addition-fragmentation chain-transfer (RAFT) polymerization. They possess a hydrophilic shell made of polycationic 4-vinyl-N-methylpyridinium iodide P($4VPMe^+I^-$) chains, a triphenylphosphine oxide (TPPO)-functionalized polystyrene core and are crosslinked at the inner end of the polystyrene chains by diethylene glycol dimethacrylate (DEGDMA) (TPPO@CCM-C). Ex-$situ$ synthesized RhNPs readily cross the hydrophilic shell and remain anchored within the CCM nanoreactor cores. The RhNP-loaded TPPO@CCM-C latex was applied as catalyst in the hydrogenation of styrene under mild conditions with complete selectivity towards ethylbenzene and average turnover frequency (TOF) up to 12000 h^{-1}, corresponding to a corrected TOF (cTOF) up to 16800 h^{-1} based on only surface atoms of the RhNPs. Moreover, the catalytic phase proved recyclable after product extraction with diethyl ether, demonstrating efficient retention of the RhNPs by the core TPPO ligands. Although the activity decreased after the first catalytic run, it converged to a stable average TOF of $ca.$ ~1025 h^{-1} (cTOF of $ca.$ ~1440 h^{-1}), which was similar to that of an extensively pre-washed RhNP-TPPO@CCM-C latex. This phenomenon is attributed to a promoter effect of adsorbed ligands, which were used as stabilizer for the RhNPs synthesis and were gradually removed during the work-up washings between recycles.

1. Introduction

The catalyzed transformation of organic compounds with metal nanoparticles (MNPs) [1] in micellar systems [2,3] combines the advantages of homogeneous and heterogeneous catalysis, including high activity, selectivity, and durability [4]. The MNPs provide a high surface to volume ratio resulting in a high number of potential catalytic sites [5], and the metal surface can be stabilized by appropriate ligands, similarly to molecular complexes. The confinement of MNPs inside a matrix (e.g., metal oxides, carbonaceous or polymeric materials) can further improve stability and catalytic performance. In particular, polymer-supported MNPs [6] have received significant attention in catalysis because of facile catalyst recovery and reuse. With such systems, using water as a solvent or dispersant phase yields aqueous biphasic systems [4,7,8] where simple phase separation facilitates catalyst recovery and recycling and allows reducing the use of volatile

* Corresponding author.
** Corresponding author. CNRS, LCC (Laboratoire de Chimie de Coordination), Université de Toulouse, UPS, INPT, 205 Route de Narbonne, BP 44099, F-31077, Toulouse, Cedex 4, France
*** Corresponding author.
**** Corresponding author.
E-mail addresses: rinaldo.poli@lcc-toulouse.fr (R. Poli), ar@kemi.dtu.dk (A. Riisager), karine.philippot@lcc-toulouse.fr (K. Philippot), eric.manoury@lcc-toulouse.fr (E. Manoury).

organic solvents and energy-intensive distillations, with a positive impact on the environment in the spirit of green chemistry. However, when the catalyst has low solubility in the organic reactant/product phase and the reactant has low solubility in water, the reaction may be limited to the organic/water interface and suffer from mass-transport restrictions. The use of surfactants or micellar systems can improve the mass-transport kinetics in biphasic aqueous/organic reactions by increasing the catalyst and substrate concentrations in the reaction zone [2,3,8,9]. Anchoring the catalyst in the hydrophobic cores of micelles permits to increase the local concentration of both catalyst and substrate and reduce the impact of mass transfer, provided the mass transport between the micellar cores and the bulk organic phase is facile. When the micelles are kinetically inert (slow exchange with the free surfactant in solution) or when they are rendered unimolecular by shell- or core-crosslinking, they operate as individual catalytic nanoreactors [10–12].

Some of us have developed synthetic protocols towards highly modular core-crosslinked micelles (CCMs) [13–20] as stable aqueous dispersions with a high polymer content (>20 wt%), by reversible addition-fragmentation chain-transfer (RAFT) polymerization [21]. The first generation of CCMs displayed a neutral shell (CCM-N) made of random copolymer blocks of poly(ethylene oxide) (PEO) methacrylate and methacrylic acid [14]. Analogous CCMs with a polycationic shell (CCM-C) of homopolymer blocks of 4-vinyl-*N*-methylpyridinium iodide (4VPMe$^+$I$^-$) were also prepared [15] (Fig. 1). All CCMs developed so far have a polystyrene-based core with diethylene glycol dimethacrylate (DEGDMA) as crosslinker, but have been functionalized with different core-linked ligands, providing L@CCM nanoreactors with L = triphenylphosphine (TPP) [13,16,19,22], bis(4-methoxyphenyl)phenylphosphine [12], nixantphos [14], and *N*-heterocyclic carbene [18]. Molecular pre-catalysts (e.g., [Rh(acac)(CO)$_2$] or [RhCl(COD)]$_2$; acac = acetylacetonate, COD = 1,5-cyclooctadiene) were successfully fixated in the CCM cores by ligand coordination, generating catalytic nanoreactors for aqueous biphasic olefin hydroformylation [14,20,23,24] and hydrogenation [16,18,19].

L@CCM nanoreactors were further applied to the confinement of RhNPs, using TPP@CCMs (RhNP-TPP@CCM) based on both CCM-N and CCM-C. The RhNPs were formed *in-situ* after loading the CCMs with the [RhCl(COD)]$_2$ molecular precursor, followed by reduction of the resulting core-anchored [RhCl(COD)(TPP@CCM)] with H$_2$. The obtained RhNP-TPP@CCM were then applied to the aqueous biphasic hydrogenation of model substrates [19]. Despite very good catalytic performances, two unexpected issues arose. When using the TPP@CCM-N nanoreactors, migration of the RhNPs towards the outer shell was observed under catalysis conditions, likely due to competition between the shell PEO chains and the core TPP ligands for the interaction with the RhNPs surface. Conversely, the RhNPs remained

well-confined in the TPP@CCM-C nanoreactors and could be efficiently recycled in catalytic hydrogenation, provided toluene was used as extraction solvent after each reaction run. When using diethyl ether as extraction solvent, on the other hand, the RhNPs were also extracted from the core of the TPP@CCM-C nanoreactors during catalyst recovery and recycling. This result suggested that the oxygen-containing diethyl ether, like the PEO on the CCM-N shell, has greater affinity for binding to the RhNPs surface than TPP, whereas the opposite is true in the coordination chemistry of Rh^I (e.g., [RhCl(COD)]$_2$). Based on this hypothesis, new L@CCM nanoreactors with triphenylphosphine oxide (TPPO) ligands as oxygen-based RhNP-anchoring core functions have been developed. The present contribution thus describes the synthesis and characterization of a novel TPPO@CCM-C polymer latex, its loading with preformed RhNPs, and the application of the resulting RhNP-TPPO@CCM-C nanoreactors in the catalytic hydrogenation of styrene under aqueous biphasic conditions.

2. Materials and methods

2.1. General methods

All manipulations were carried out using Schlenk-line techniques under an inert atmosphere of dry argon. (4-Styryl)diphenylphosphine (SDPP, 97%, Aldrich), 4,4′-azobis (4-cyanopentanoic acid) (ACPA, >98%, Fluka), diethylene glycol dimethacrylate (DEGDMA, 95%, Sigma-Aldrich) and hydrogen (99.999%, Air Liquide) were used as received. 4-Vinyl pyridine (4VP, 95%, Sigma) and styrene (St, 99%, Acros) were distilled under reduced pressure prior to use. The RAFT agent 4-cyano-4-thiothiopropylsulfanyl pentanoic acid (CTPPA) or R$_0$-SC(S)S*n*Pr (R$_0$=C(CH$_3$)(CN)CH$_2$CH$_2$COOH) [17] and 1-methyl-4-vinyl-pyridinium iodide (4VPMe$^+$I$^-$) were prepared according to previously described methods [25]. The compound (4-styryl)diphenylphosphine oxide (SDPPO) was synthesized following a literature procedure [26]. The deionized water used for the syntheses and dynamic light scattering (DLS) analyses was obtained from a Purelab Classic UV system (Elga Lab-Water). The autoclaves used for the syntheses of RhNPs and for the hydrogenation catalysis had a volume of 15 mL and were homebuilt.

2.2. Characterization techniques

2.2.1. Nuclear magnetic resonance (NMR) spectroscopy

Liquid NMR spectra were recorded in 5 mm diameter tubes at 25 °C on Bruker Avance III 300 or 400 MHz spectrometers. The ^{1}H and ^{13}C chemical shifts were determined using the residual peak of the deuterated solvent as internal standard and are reported in ppm (δ) relative to tetramethylsilane. Peaks are labelled as singlet (s), doublet (d), triplet (t), quadruplet (q), multiplet (m) and broad (br). For the synthesis of the
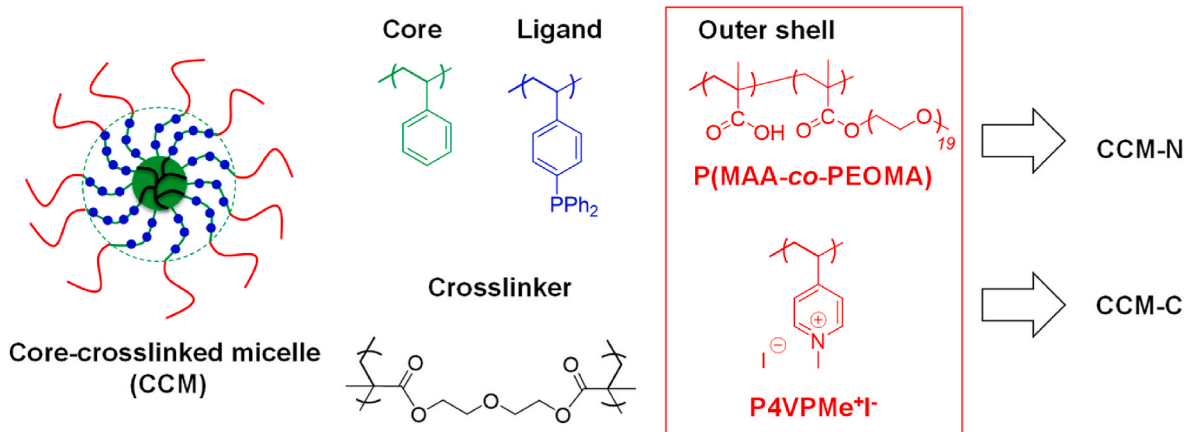

Fig. 1. TPP-functionalized core-crosslinked micelles (TPP@CCM) previously used as support for RhNPs in aqueous biphasic hydrogenation catalysis [16,18,19].

P4VP-SC(S)SnPr macroRAFT agent, the monomer conversion was monitored by ^{1}H NMR in DMSO-d_6 at 25 °C by the relative integration of the protons of the internal reference (1,3,5-trioxane, δ 5.20) and the vinylic protons of 4VP (at δ 5.4 and 5.9).

2.2.2. Dynamic light scattering (DLS)

The z-average diameters of the polymer particles (Dz) and the polydispersity index (PDI) were obtained with a Malvern Zetasizer NanoZS equipped with a He–Ne laser (λ = 633 nm), operating at 25 °C. Samples were analyzed after dilution (with deionized water), either unfiltered or after filtration through a 0.45 µm pore-size membrane. The procedure without filtration allowed verification of the presence of agglomerates. Each value was the average of five measurements. In each figure, the curves labelled N, V and I represent the instrumental responses in number, volume, and intensity, respectively.

2.2.3. Transmission electron microscopy (TEM)

Morphological analyses of copolymer micelles and RhNPs were carried out with a JEOL JEM 1400 transmission electron microscope working at 120 kV (Centre de Microcaractérisation Raimond Castaing, UAR 3623, Toulouse, France). Diluted aqueous samples were dropped on a formvar/carbon-coated copper grid and dried under vacuum for 24 h before analysis.

2.2.4. Gas chromatography (GC)

Quantitative determination of products and of residual substrates in organic phases after catalysis were conducted using an Agilent 6890 N gas chromatograph equipped with a HP-5MS capillary column (30 m × 250 µm × 0.25 µm) and a flame ionization detector (FID), using helium as the carrier gas. The peak assignment was assisted by separate GC mass spectrometry (GC-MS) analysis on an Agilent 6850-5975C instrument.

2.2.5. Inductive coupled plasma mass spectrometry (ICP-MS)

Rh metal leaching into the organic phase after catalysis was quantified by high-resolution ICP-MS using a XR Thermo Scientific Element (Observatoire Midi-Pyrénées (OMP), Géosciences Environnement Toulouse, France). For the sample preparation, the recovered organic phase was diluted in water using a 104 volumetric dilution factor, high enough to ensure complete dissolution. In practice, a 100 mL volumetric flask was filled 2/3 with Milli-Q water, then 10 µL of the organic product phase was introduced using a precision pipette. The borders were rinsed, and the flask was introduced into an ultrasonic bath for 15 min. The dilution was then completed with Milli-Q water to the 100 mL mark, followed by further sonication for 45 min. Standards were prepared using [RhCl(COD)]$_2$ dissolved in toluene, attaining Rh concentrations in aqueous solution in the 1–100 ppt range. The relative standard deviation on the measurements used for the calibration was 3%.

2.3. Synthesis of P(4VPMe$^+$I$^-$)-b-PS-b-P(St-co-SDPPO) amphiphilic block copolymer

The first three steps of the polymer synthesis were carried out as described in the previous contribution [17], using CTPPA (0.201 g, 0.72 mmol), 4VP (11.7 mL, 11.4 g, 101 mmol; 4VP/CTPPA = 140), styrene (4.14 mL, 3.76 g, 36.2 mmol, 50 equiv. per chain), and CH$_3$I (63.05 mL, 143.7 g, 101 mmol, ca. 10 equiv. *vs.* 4VP), and yielded 10.54 g of macromolecules with average stoichiometry [R$_0$-(4VPMe-$^+$I$^-$)$_{140}$-b-St$_{50}$-SC(S)SPr]·14DMF (formula determined by ^{1}H NMR in DMSO-d_6, molar mass = 41094 g mol^{-1}) (yield = 63.5%).

2.3.1. Preparation of R$_0$-(4VPMe$^+$I$^-$)$_{140}$-b-St$_{50}$-b-(St$_{0.9}$-co-SDPPO$_{0.1}$)$_{300}$-SC(S)SnPr (chain extension with styrene and SDPPO, step 4)

A portion of the [R$_0$-(4VPMe$^+$I$^-$)$_{140}$-b-St$_{50}$-SC(S)SnPr]·14DMF polymer resulting from the three step synthesis above (1.0 g, 24.3 µmol) was dissolved in 19 mL of degassed water to afford a pale yellow opalescent dispersion. To this mixture was added 1,3,5-trioxane (26.3 mg, 0.29 mmol), degassed styrene (0.75 mL, 0.68 g, 6.55 mmol, 270 equiv. per chain) and SDPPO (0.22 g, 0.73 mmol, 30 equiv. per chain). Then a degassed ACPA/NaHCO$_3$ (14 mg/14 mg) stock solution (0.7 mL, 14.01 mg ACPA, 5 µmol) was added and the resulting reaction mixture was stirred at 80 °C for 8.5 h, yielding a white opalescent stable dispersion. The resulting polymer, R$_0$-(4VPMe$^+$I$^-$)$_{140}$-b-St$_{50}$-b-(St$_{0.9}$-co-SDPPO$_{0.1}$)$_{300}$-SC(S)SnPr, has a theoretical molar mass of 78337 g mol^{-1}.

2.3.2. Preparation of R$_0$-(4VPMe$^+$I$^-$)$_{140}$-b-St$_{50}$-b-(St$_{0.9}$-co-SDPPO$_{0.1}$)$_{300}$-b-(St$_{0.9}$-co-DEGDMA$_{0.1}$)$_{150}$-SC(S)SnPr core-crosslinked micelles (CCM-C latex)

To a Schlenk tube containing the entire aqueous suspension of the R$_0$-(4VPMe$^+$I$^-$)$_{140}$-b-St$_{50}$-b-(St$_{0.9}$-co-SDPPO$_{0.1}$)$_{300}$-SC(S)SnPr polymer prepared in step 4 were successively added degassed styrene (0.35 g, 3.36 mmol, 138 equiv. per chain), DEGDMA (0.09 g, 0.36 mmol, 15 equiv. per chain), and a degassed ACPA/NaHCO$_3$ stock solution (0.7 mL, 14.01 mg ACPA, 5 µmol). The resulting reaction mixture was stirred at 80 °C for 8.5 h, resulting in the complete conversion of both monomers (followed by ^{1}H NMR in DMSO-d_6 on periodically withdrawn aliquots of reaction mixture). The final polymer latex has a theoretical molar mass (per RAFT CTA) of 96835 g mol^{-1} with a polymer content of 12.3 wt%.

2.4. Synthesis of preformed RhNPs and of RhNP-TPPO@CCM-C latex

2.4.1. Synthesis of RhNPs stabilized with pyridine and TPP

[RhCl(COD)]$_2$ (5.45 mg, 11.6 µmol), TPP (5.8 mg, 22.1 µmol, 1 equiv. per Rh) and pyridine (2 µL, 1.75 mg, 22.1 µmol, 1 equiv. per Rh), and 0.5 mL of toluene were mixed by magnetic stirring for 5 min in a Schlenk tube and then transferred to a glass vial (40 × 20 mm), which was placed into an autoclave. The autoclave was then charged with 20 bar of H$_2$ and placed in an aluminum heating block at 60 °C. After stirring (1200 rpm) for 20 h, the autoclave was carefully depressurized and the vial containing a black colloidal suspension of RhNPs in toluene was removed under argon.

2.4.2. Synthesis of RhNP-TPPO@CCM-C latex

The prepared CCM-C latex (1 mL, 51.14 µmol of TPPO ligands) was mixed with water (3 mL) and toluene (4 mL) in a Schlenk tube, and magnetically stirred for 5 min to induce the CCM core swelling. Then, 0.5 mL of the separately prepared colloidal suspension of RhNPs (11.6 µmol, TPPO/Rh= ratio of 4/1) in toluene was added and the mixture was vigorously stirred (1200 rpm) at room temperature for 5 min, whereafter the aqueous phase became greyish and the toluene phase completely colorless (stirring was stopped at regular intervals to assess the reaction progress with phase-separation occurring within <1 min). The resulting RhNP-TPPO@CCM-C latex had a volume of 5.5 mL.

2.5. Hydrogenation catalysis

2.5.1. Aqueous biphasic hydrogenation

To a glass vial containing the RhNP@CCM-C latex (0.5 mL, 4.9 µmol of TPPO ligands, 1.05 µmol of Rh) were added the desired amounts of styrene (see Results and Discussion) and decane (internal standard; substrate/internal standard molar ratio *ca.* 4/1). The vial was then placed inside a custom-made autoclave, charged with 20 bar of H$_2$ and placed in an aluminum heating block at the desired temperature (see Results and Discussion) with magnetic stirring (1200 rpm) for a chosen reaction time. After the set time the stirring was stopped, the autoclave was slowly vented, the vial was removed (under argon) and the reaction mixture was allowed to phase separate. After completed phase separation, the latex was extracted with diethyl ether or toluene (3 × 0.3 mL), applying 5 min of stirring (1200 rpm) followed by 5 min for phase separation without stirring for each extraction (these operations were carried out in air). Lastly, the combined organic phases were analyzed by GC and the catalyst activity calculated as turnover frequency (TOF) and corrected TOF (cTOF) (see Supporting Information for details).

2.5.2. Catalyst recycling experiments

After the product separation and extraction, the vial containing the RhNP@CMM-C latex from the hydrogenation experiment was charged directly with fresh substrate (same amount as in the initial run), followed by a new catalytic run and then by the product separation procedure according to the above-described protocol. All catalytic results were generally reproduced with ±5%.

3. Results and Discussion

3.1. Polymer synthesis and characterization

The synthesis of the new TPPO@CCM-C polymer was carried out following the same strategy used for the preparation of the closely related TPP@CCM-C polymer (Scheme 1). The target degrees of polymerization of each block were kept identical to those of TPP@CCM-C, as they were already optimized to provide stable latexes with a narrow particle size distribution [16,17]. Thus, the first three steps leading to the synthesis of the amphiphilic diblock macroRAFT agent, R_0-(VPMe-$^+$I$^-$)$_{140}$-b-St$_{50}$-SC(S)SnPr, isolated as a stable solid and redispersed in water, were the same as in the TPP@CCM-C synthesis [17]. They involved the homogeneous RAFT polymerization of 4VP with CTPPA, R_0SC(S)SnPr where R_0 = CMe(CN)CH$_2$CH$_2$COOH), as transfer agent, forming R_0–4VP$_{140}$-SC(S)SnPr (step 1), then chain extension with a short polystyrene block (average degree of polymerization of 50) forming an R_0-VP$_{140}$-b-St$_{50}$-SC(S)SnPr diblock copolymer (step 2), and quaternization of the pyridine N-atoms with MeI (step 3).

The fourth step was a further chain extension of the R_0-(VPMe$^+$I$^-$)$_{140}$-b-St$_{50}$-SC(S)SnPr macroRAFT agent with a longer hydrophobic block (average degree of polymerization of 300) consisting of a statistical copolymer of styrene and a TPPO-functionalized styrene, namely SDPPO (4-styryldiphenylphosphine oxide) [12,27,28] (90/10 ratio), which was obtained by oxidation of SDPP with H$_2$O$_2$ (Figs. S1–S3). This monomer has previously been homopolymerized [12, 27,28] and copolymerized with styrene [29] and 9-(4-vinyl-phenyl)-9H-carbazole [30] by free radical polymerization, but not using the RAFT approach. All the polymerization steps were followed to completion (full consumption of monomers) by ^{1}H NMR (Figs. S4 and S5), and the generated R_0-(VPMe$^+$I$^-$)$_{140}$-b-St$_{50}$-b-(St$_{0.9}$-co-SDPPO$_{0.1}$)$_{300}$-SC(S)SnPr amphiphilic macromolecules self-assembled in the form of micelles. The resulting latex remained well-dispersed over more than five months (Fig. S6).

The spherical micelles of the amphiphilic diblock copolymer produced by step 4 had an average size of ca. 65 nm, as shown by DLS

analysis (Fig. 2a). These micelles were then crosslinked in a final step with DEGDMA (15 equiv. per chain), diluted with additional styrene (135 equiv. per chain), to yield the final product, R_0-(VPMe$^+$I$^-$)$_{140}$-b-St$_{50}$-b-(St$_{0.9}$-co-SDPPO$_{0.1}$)$_{300}$-b-(St$_{0.9}$-co-DEGDMA$_{0.1}$)$_{150}$-SC(S)SnPr (TPPO@CCM-C), with a 10% crosslink density in the inner crosslinked core. The final TPPO@CCM-C polymer particles had spherical morphology and a slightly larger diameter (98.5 nm) than the intermediate micelles, as shown by DLS (Fig. 2c) and TEM (Fig. 2d) analyses. The size distribution became narrower and the D_z of the distribution was slightly reduced after swelling with CHCl$_3$. This size reduction phenomenon upon swelling was also observed for related CCMs with an anionic shell (TPP@CCM-A) and was attributed to the dominant effect of micelles disaggregation rather than core swelling, which would cause an increase in average size [22]. Accordingly, the intensity profile in Fig. 2b, which is more sensitive to the larger size micelles, became significantly narrower and shifted to lower values upon swelling.

3.2. Synthesis of RhNP-TPPO@CCM-C

The first attempt to produce RhNP-TPPO@CCM-C consisted in loading the CCM-C with [RhCl(COD)]$_2$, in order to generate a core-anchored [RhCl(COD)(TPPO@CCM-C)] complex that could be reduced to RhNPs by H$_2$, following the procedure previously developed to generate RhNPs embedded in TPP@CCM-C [19]. Mononuclear complexes with the [Rh(η^2:η^2-diene)Cl(L)] stoichiometry (e.g. diene = COD, norbornadiene) where L is an O-atom donor ligand are rare [31–34], but the [RhCl(COD)(TPPO)] complex has been described [35–37]. Nevertheless, this method proved unsuccessful as the organic phase was observed to remain yellow-colored, even after heating the reaction mixture at 60 °C for 1 h or after stirring at room temperature for 24 h. This indicates that the formation of a Rh^I-TPPO@CCM-C complex in the polymer core by cleavage of the di-μ-Cl-bridge moiety in [RhCl(COD)]$_2$ is not favorable under the applied conditions.

Therefore, an alternative strategy involving *ex-situ* synthesis of RhNPs and their subsequent transfer to the TPPO@CCM-C nanoreactors was considered. For this purpose, the RhNPs were produced by reduction of [RhCl(COD)]$_2$ with H$_2$ in the presence of pyridine and TPP as stabilizing ligands. This ligand combination was inspired by previous reports, which showed TPP to be an effective stabilizer to produce ultrasmall RhNPs [6,38–41], while pyridine was used for the formation of RhNPs in ionic liquids [40]. The RhNPs synthesis was conducted in toluene, which has a high swelling power for the polystyrene-based CCM-C core [42]. The optimized conditions (TPP/Pyridine/Rh = 1/1/1, 60 °C, 20 bar H$_2$, 20 h) led to a stable, black colloidal suspension
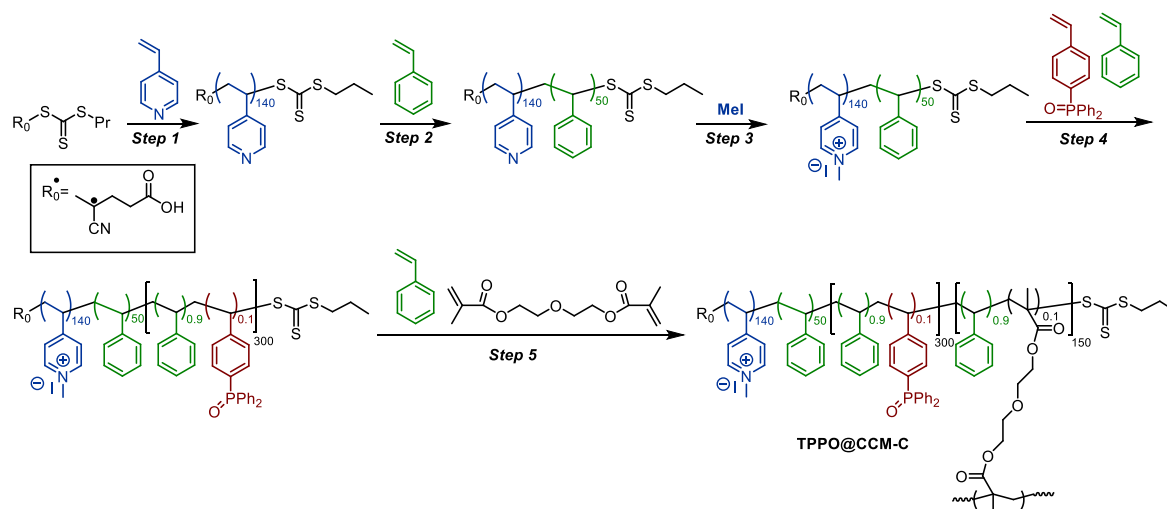
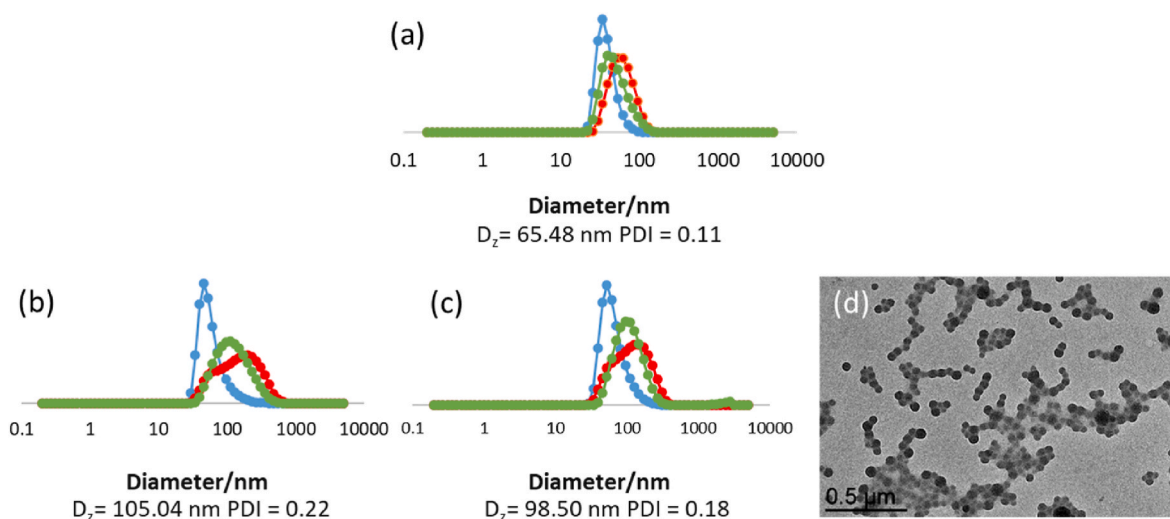**Scheme 1.** Synthesis route of the TPPO@CCM-C polymer.

Fig. 2. DLS size distributions of aqueous dispersions of (a) the diblock R_0-(VPMe$^+$I$^-$)$_{140}$-b-St$_{50}$-b-(St$_{0.9}$-co-SDPPO$_{0.1}$)$_{300}$-b-SC(S)SnPr micelles and of TPPO@CCM-C (b) before and (c) after swelling with CHCl$_3$. Color coding: number (blue), volume (green) and intensity (red). d) TEM image of the TPPO@CCM-C.

of RhNPs, which displayed a mean diameter of 1.2 ± 0.4 nm and a narrow size distribution (Fig. 3).

Addition of the RhNPs colloidal suspension to the TPPO@CCM-C latex (P/Rh = 4/1) led to a fast and complete discoloration of the toluene phase while the latex became grey. This indicated the successful transfer of the RhNPs across the P(4VPMe$^+$I$^-$) hydrophilic shell of the CCM-C and their anchoring to the TPPO functions in the polymer cores, which was corroborated by DLS and TEM characterization of the final RhNP-TPPO@CCM-C (Fig. 4). The DLS analysis showed that the CCM-C polymer particles had very similar average size and size distribution before and after the loading with the RhNPs. The TEM analysis confirmed that the RhNPs were located inside the polymer particles and indicated an average size of ca. 1.5 ± 0.4 nm. Despite the presence of the polymer that renders the measurement more difficult, it can be concluded that the RhNPs had quite similar sizes to the as-synthesized RhNPs (Fig. 3). This result indicates that the RhNPs are not significantly altered by the ligand exchange in the CCM-C core.

3.3. Hydrogenation of styrene

3.3.1. Hydrogenation with colloidal suspension of RhNPs in toluene

The catalytic activity of the toluene colloidal suspension of TPP/pyridine-stabilized RhNPs was evaluated for the hydrogenation of styrene under mild reaction conditions (20 bar H$_2$, 25 °C, 0.25 h) with styrene/Rh of ~10000/1. A styrene conversion of ~90% was observed, corresponding to an average TOF of ~36900 h^{-1} (cTOF of ~40700 h^{-1}), with complete selectivity towards ethylbenzene (EB). This catalytic performance is superior to those previously described with RhNPs stabilized by TPP (TOF of ~6000 h^{-1}) or diphosphate ligands (TOF of

~24000 h^{-1}) under 40 bar H$_2$ in heptane at room temperature and 0.25 h [38]. The selectivity in favor of EB is not suprising, because previous investigations have underlined the tuneable properties of RhNPs [38,39, 43–45] and the role of their size in controlling the selectivity of styrene hydrogenation. For instance, RhNPs with size in the 2–10 nm range exhibited a propensity for ring hydrogenation [46]. Conversely, selective hydrogenation to EB occurred under mild conditions using RhNPs with an average diameter of 1.5 nm [47], though benzene ring hydrogenation was observed under more forcing conditions. The dependence of reaction selectivities on the metal NP size has also been highlighted in other contributions [48–51].

3.3.2. Hydrogenation with RhNP-TPPO@CCM-C latex under biphasic conditions

Next, the RhNP-TPPO@CCM-C latex was applied to the aqueous biphasic hydrogenation of styrene under the same temperature and pressure conditions as with the colloidal RhNPs suspension (20 bar H$_2$, 25 °C), with a styrene/Rh ratio of ~2000/1, at different reaction times (Fig. 5). Since styrene is a good solvent for polystyrene, no vectorizing solvent was needed and the hydrogenation was carried out with the neat substrate [16,19] using an agitation of 1200 rpm to ensure a good external mass transfer.

A nearly complete styrene conversion (~94%) was obtained in only 0.25 h, corresponding to an average TOF of 7733 h^{-1} (cTOF of 9850 h^{-1}), with an excellent selectivity (>99%) towards EB (Table 1, entry 1). This catalytic performance is superior to that previously achieved with RhNPs embedded in the TPP@CCM-C [19,38,45] (Table S2). This difference may be related to the smaller size of the *ex-situ* synthesized TPP/pyridine-stabilized RhNPs used to get RhNP-TPPO@CCM-C
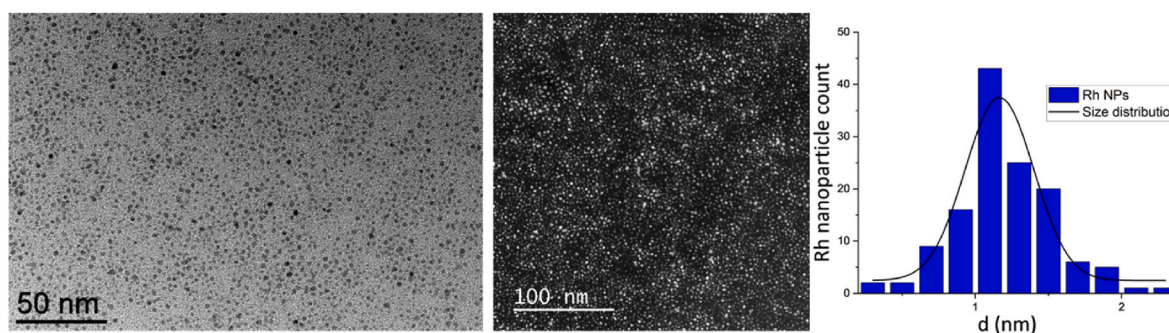

Fig. 3. TEM images of RhNPs stabilized by TPP and pyridine (left) and the corresponding size distribution histogram (d_m = 1.2 ± 0.4 nm) (right).
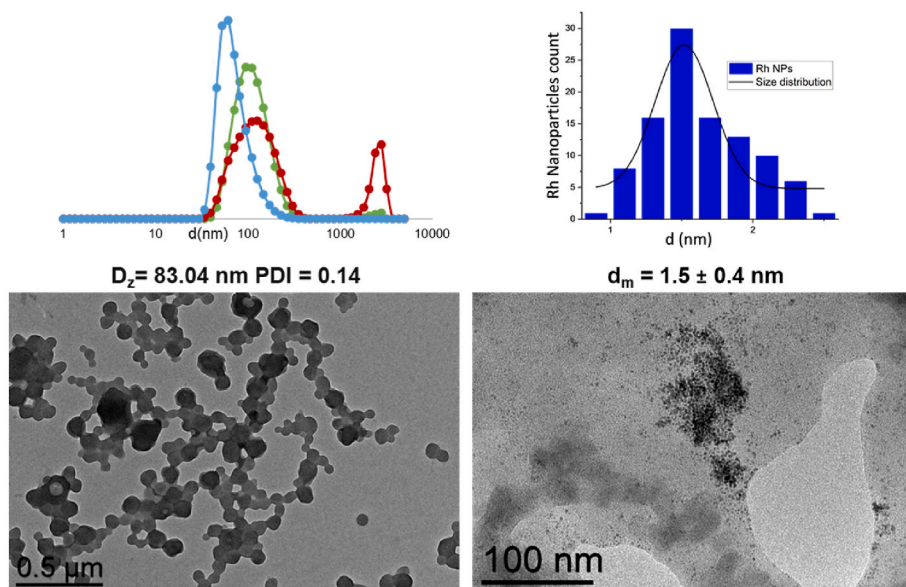
Fig. 4. DLS and TEM analysis of Rh-TPPO@CCM-C showing the micelle size distribution (top left), the RhNP size distribution (top right) and TEM images of Rh-TPPO@CCM-C (bottom). Color coding: number (blue), volume (green) and intensity (red).
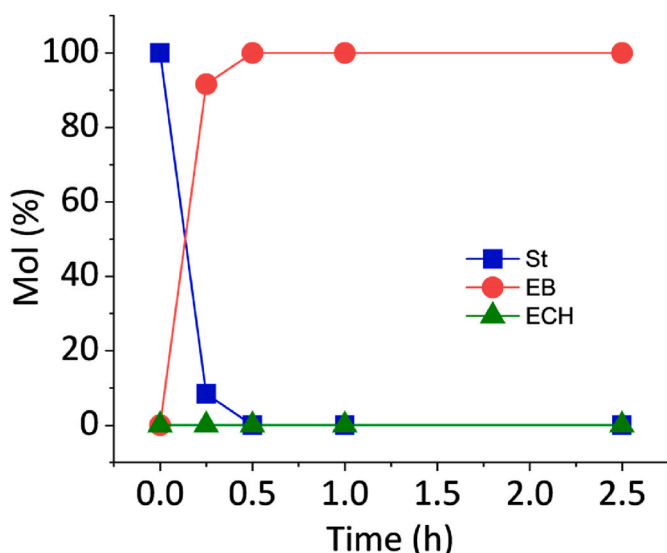

Fig. 5. Time plot for the aqueous biphasic hydrogenation of styrene using RhNPs-TPPO@CCM-C. Reaction conditions: Styrene/Rh of ~2000/1, 20 bar H_2, 25 °C.

compared to the *in-situ* synthesized TPP@CCMC-stabilized RhNPs in RhNP-TPP@CCM-C (1.2 nm *vs.* <5 nm). However, additional experiments indicated that the adsorbed TPP and pyridine stabilizers in the RhNP-TPPO@CCM-C catalyst also played a role (*vide infra*). An increase of the styrene/Rh ratio resulted in good and reproducible conversions within 0.25 h of 53% (styrene/Rh of ~5000/1) and 24% (styrene/Rh of ~10000/1), corresponding to average TOFs of 10547 and 9062 h^{-1} (cTOFs of 14300 and 12440 h^{-1}), respectively, again with full selectivity towards EB (Table 1, entries 2 and 3). Upon stopping the stirring, a rapid phase separation (<3 min) was observed in all reactions, thus facilitating the product separation and catalyst recovery, as already reported for the RhNP-TPP@CCM-C nanoreactors featuring the same outer shell [19].

The recycling of the catalytic RhNP-TPPO@CCM-C latex was evaluated in two series of experiments at a fixed styrene/Rh ratio of ~5000/1, by extracting the reaction products with diethyl ether or toluene,

respectively, prior to the addition of a new batch of substrate for the next catalytic run. The extraction protocol was identical to that used in the previously reported recycling studies with the RhNP-TPP@CCM-C [19] and with the molecular Rh[I]-TPP@CCM [16] catalytic systems. The first catalytic runs yielded styrene conversion of 53% in 0.25 h. However, a gradual decrease in conversion, from 53% to *ca.* 9–15%, was witnessed after the fifth run for both series of recycles, using either toluene or diethyl ether for product extraction (Fig. 6). The ICP-MS analyses showed only a cumulative loss of ~2% of the catalyst inventory after the five catalytic runs when using diethyl ether as extraction solvent, indicating that the activity decrease was not caused by metal leaching and mechanical loss of latex (SI Table S1). Moreover, after catalyst separation, whether toluene or diethyl ether was used as the extraction solvent, the organic phase was completely transparent and colorless while the aqueous phase remained grey, thus indicating the retention of the RhNPs in the CCM-C latex. In both cases, the TEM images obtained for the RhNP-TPPO@CCM-C catalyst after the fifth run evidenced a preserved confinement of the RhNPs in the CCM-C cores with well dispersed RhNPs. These results indicate that the interaction of the RhNPs with the core-linked TPPO ligands is sufficiently strong to retain them within the hydrophobic CCM-C cores, validating the initial hypothesis of the superior efficiency of oxygen-coordinating ligands. Though an artifact cannot be ruled out due to the less defined polymer-embedded RhNPs, a notable change was an increase of the particle size (from 1.5 ± 0.4 nm to 2.2 ± 0.9 nm after the fifth catalytic run) (Fig. S7). This may indicate a slight growth or aggregation of the NPs. However, given that the standard deviation value is larger than the size change (0.9 nm *vs.* 0.7 nm), the NPs can also be considered as to be in a similar size range, thus the interpretation of the activity drop as a result of a size change does not appear satisfactory.

Given that no significant metal leaching was detected and that no substantial NP agglomeration that may lead to loss of active surface was observed, progressive passivation of the RhNPs surface by rhodium oxide formation could be responsible for the decrease in catalytic performance over subsequent recycles. To verify this hypothesis, the catalyst recycling with product extraction by diethyl ether was completed under an inert argon atmosphere. In addition, the recovered RhNP-TPPO@CCM-C phase was treated with H_2 (20 bar H_2, 25 °C, 1 h) prior to each catalytic run, to remove any rhodium oxide layer. Despite these precautions in the recycling experiments, the styrene conversion still decreased to 10% along the five runs (Fig. 7). The similarity of these

Table 1
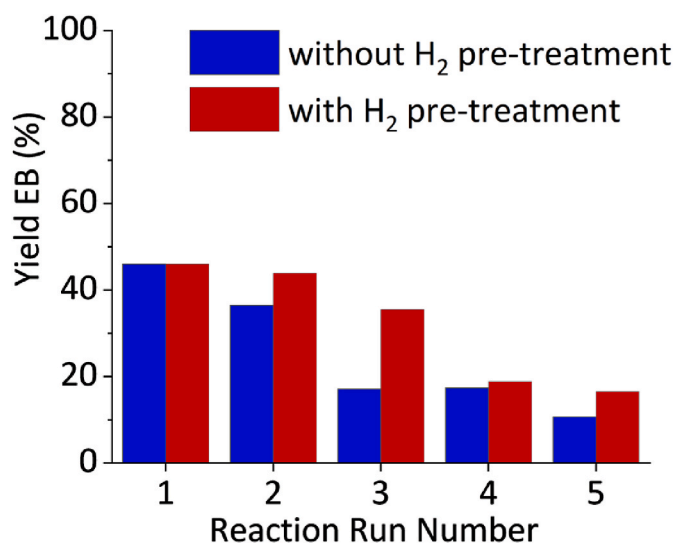Hydrogenation of styrene using RhNP-TPPO@CCM-C.[a]
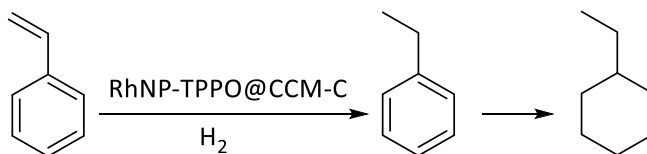
Entry	Molar ratio of styrene/Rh	Conversion (%)	Product Yield (%)		TOF (h^{-1})[b]
			Ethylbenzene	Ethylcyclohexane	
1	2056/1	94	94	<0.1	7733 (9850)
2	4975/1	53	52	<0.1	10547 (14300)
3	9440/1	24	23	<0.1	9062 (12440)

[a] Reaction conditions: 20 bar H_2, 25 °C, 0.25 h.
[b] Average values over the duration of the reaction, expressed as moles of substrate converted per moles of Rh in the catalyst per hour (TOF) or as moles of substrate converted per moles of surface Rh atoms per hour (cTOF, in parenthesis).
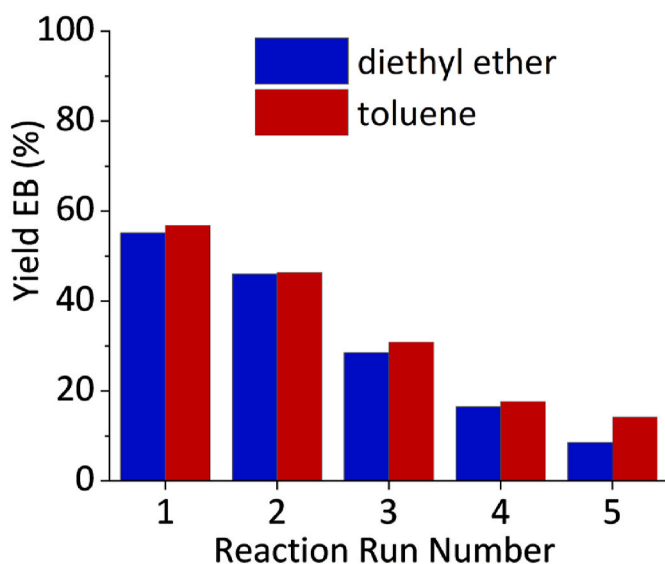
Fig. 6. Reuse of RhNP-TPPO@CCM-C in five catalytic runs of styrene hydrogenation with intermediate product extraction by diethyl ether (blue) and toluene (red). Reaction conditions: Styrene/Rh of ~5000/1, 20 bar H_2, 25 °C, 0.25 h.

Fig. 7. Reuse of RhNP-TPPO@CCM-C in five catalytic runs of styrene hydrogenation with product extraction by diethyl ether under argon with and without intermediate H_2 treatment (20 bar H_2, 25 °C, 1 h). Reaction conditions: Styrene/Rh of ~5000/1, 20 bar H_2, 25 °C, 0.25 h.

results to those achieved without inert atmosphere and reductive treatment (Fig. 6), suggests that passivation of the RhNPs was not the unique reason behind the decrease in the activity.

A reduction of the anchoring TPPO ligands to TPP by H_2, catalyzed by the RhNPs, is another possible hypothesis to explain the observed activity decrease, assuming a lower activity for RhNP-TPP relative to RhNP-TPPO. To assess this hypothesis, a toluene solution of TPPO- and TPP/pyridine-stabilized RhNPs (TPPO/Rh = 8/1) was exposed to H_2 (20 bar) at 60 °C for 22 h. A ^{31}P NMR monitoring of the solution revealed no detectable TPPO reduction (Fig. S8). This result seems to indicate that the TPPO ligands in the CCM-C core most likely remained unchanged under the conditions of the aqueous biphasic styrene reduction catalysis. The absence of TPPO reduction to TPP is also indirectly indicated by the demonstrated ability of diethyl ether to extract the RhNPs from the RhNP-TPP@CCM-C [19], whereas the TEM analysis (*vide supra*) shows that the RhNPs are well-retained in the micellar core.

A final working hypothesis is that the stabilizers used for the *ex-situ* synthesis of RhNPs (TPP/pyridine) partially remained in the TPPO@CCM-C core after loading and promoted the catalytic activity of the RhNPs, and that the activity gradually decreased as these stabilizers/

promoters were continuously washed out during the work-up for catalyst recovering and recycling. This hypothesis was tested by washing the fresh RhNP-TPPO@CCM-C latex, after RhNPs loading, three times with diethyl ether prior to use in catalysis. A GC-MS analysis of the diethyl ether extracts showed two peaks with MS spectra yielding molecular ions at *m/z* 112 and 83, respectively (Fig. S9). These peaks match cyclooctane and tetrahydropyridine, respectively, resulting from the hydrogenation of the COD ligand from [RhCl(COD)]$_2$ and of pyridine during the *ex-situ* synthesis of the RhNPs [43,44,47]. Subsequently, five subsequent catalytic runs (all reproduced three times) were carried out (20 bar H_2, 25 °C, 1 h) (Fig. 8). The first catalytic run provided a low conversion of styrene (~6%), whereas a constant styrene conversion of *ca.* 25% was achieved in the following four runs, corresponding to an average TOF of ~1025 h^{-1} (cTOF ~1440 h^{-1}). The low conversion in the first run might indicate that an induction time would be necessary to deblock the active sites and/or the RhNPs experienced significant changes under catalytic conditions. Comparison of a series of TEM measurements performed with the diethyl ether-washed catalyst (prior to catalysis) before/after H_2 treatment and after the first and fifth catalytic runs (Fig. S10), confirmed that the RhNPs mean size indeed changed from 4.2 ± 0.2 nm to 2.2 ± 0.2 nm before and after H_2
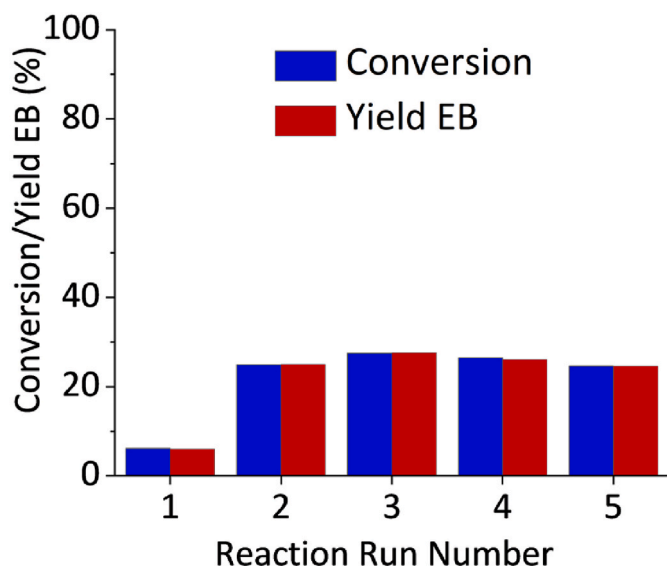
Fig. 8. Hydrogenation of styrene with RhNP-TPPO@CCM-C after three washings with diethyl ether (run 1) and recycling of the catalyst in four additional reaction runs with product extraction by diethyl ether and intermediate H_2 treatment (20 bar H_2, 25 °C, 1 h). Reaction conditions: Styrene/Rh of ~5000/1, 20 bar H_2, 25 °C, 1 h.

treatment, respectively, and was further reduced to a static size of 1.8 ± 0.1–0.3 nm after the first catalytic run. Thus, the removal of the stabilizers likely induced a slight size increase or agglomeration of the RhNPs, resulting in lower catalytic activity, as also previously reported for RhNPs in styrene hydrogenation [38,47], while the successive H_2 treatment prompted reconstruction of the NPs [41,52] possibly aided by the presence of TPPO@CCM-C. Notably, although a different reaction time was applied (1 h *vs.* 0.25 h), the styrene conversion value of *ca.* 25% obtained after the initial run is comparable to that obtained in the fourth and fifth recycles performed with intermediate product extraction by diethyl ether (Fig. 6). This suggests that the diethyl ether washings performed between the consecutive catalytic runs (Fig. 6) have a similar effect to those carried out on the fresh RhNP-TPPO@CCM-C prior to its implementation in catalysis. This indicates a possible role of the RhNP stabilizers (TPP, pyridine and tetrahydropyridine, see GC-MS results above) on the hydrogenation of styrene when they are not eliminated by solvent washings [53–56]. It is also to be noted that, as shown above, the RhNP-catalyzed styrene hydrogenation in toluene yields a much higher TOF for the RhNPs stabilized by TPP and pyridine (~3,000 h^{-1}) with respect to other RhNPs synthesized using other stabilizers, under similar experimental conditions [41]. This highlights that a careful choice of stabilizers to pre-synthesizd RhNPs for their transfer in the CCM-C, or the integration of co-ligands in the cores of CCM-C could be a way to boost the catalytic performance, but this is out of the scope of the present work.

4. Conclusions

Ultrasmall TPP/pyridine-stabilized RhNPs demonstrated excellent catalytic activity (average TOF ~36000 h^{-1}, cTOF ~40700 h^{-1}) and complete selectivity in the hydrogenation of styrene to EB under mild conditions (25 °C, 20 bar of H_2) in toluene. These NPs were successfully transferred to the TPPO-functionalized core of novel CCMs with a cationic shell synthesized by RAFT polymerization, and the resulting RhNP-TPPO@CCM-C latex proved effective in the aqueous biphasic hydrogenation of styrene. Compared to previous studies with RhNP-TPP@CCM-C, anchoring the RhNPs to the core-TPPO ligands prevented RhNPs extraction by diethyl ether. This shows that the nature of the core functional ligands of the polymer micelles is a key parameter to

improve the stability and the recycling of the catalytic latex. Although the extraction of RhNP stabilizers during the work-up between recycles induced a gradual decrease of the catalytic activity, a stable catalyst phase was obtained in several recycles with average TOF of ~1025 h^{-1} (cTOF ~1440 h^{-1}), after preliminary washing and an initial reaction run. Further investigations will focus on kinetic studies aimed at addressing the mass transfer properties, on the improvement of the catalytic performance, and on extending the nanoreactors application to the hydrogenation of other substrates, including carbonyl compounds.

Credit author statement

Chantal J. Abou-Fayssal: Investigation, Visualization, Writing - Original Draft; **Christophe Fliedel:** Validation, Writing - Review & Editing; **Rinaldo Poli:** Funding acquisition, Conceptualization, Writing - Review & Editing; **Anders Riisager:** Resources, Supervision, Writing - Review & Editing; **Karine Philippot:** Conceptualization, Resources, Supervision, Writing - Review & Editing; **Eric Manoury:** Resources, Supervision, Writing - Review & Editing.

Funding

Declaration of competing interest

The authors declare that they have no known competing financial interests or personal relationships that could have appeared to influence the work reported in this paper.

Data availability

Data will be made available on request.

Acknowledgments

Appendix A. Supplementary data

Supplementary data to this article can be found online at https://doi.org/10.1016/j.mtchem.2023.101752.

References

[1] R.L. Johnston, Metal nanoparticles and nanoalloys, in: Frontiers of Nanoscience, Elsevier Ltd, 2012, pp. 1–42, https://doi.org/10.1016/B978-0-08-096357-0.00006-6, 3.

[2] T. Shen, S. Zhou, J. Ruan, X. Chen, X. Liu, X. Ge, C. Qian, Recent advances on micellar catalysis in water, Adv. Colloid Interface Sci. 287 (2021), 102299, https://doi.org/10.1016/j.cis.2020.102299.

[3] T. Kotre, M.T. Zarka, J.O. Krause, M.R. Buchmeiser, R. Weberskirch, O. Nuyken, Design and application of amphiphilic polymeric supports for micellar catalysis, in: Macromol. Symp., 2004, pp. 203–214, https://doi.org/10.1002/masy.200451316.

[4] Boy Cornils, Catalysis from A to Z : A Concise Encyclopedia, Wiley-VCH, 2000, https://doi.org/10.1016/S1351-4180(13)70258-7.

[5] D.V. Talapin, E.V. Shevchenko, Introduction: nanoparticle chemistry, Chem. Rev. 116 (2016) 10343–10345, https://doi.org/10.1021/acs.chemrev.6b00566.

[6] M. Ibrahim, M. Wei, É. Deydier, E. Manoury, R. Poli, P. Lecante, K. Philippot, Rhodium nanoparticles stabilized by ferrocenyl-phosphine ligands: synthesis and catalytic styrene hydrogenation, Dalton Trans. 48 (2019) 6777–6786, https://doi.org/10.1039/C9DT01006H.

[7] O. Nuyken, P. Persigehl, R. Weberskirch, Amphiphilic poly(oxazoline)s - synthesis and application for micellar catalysis, Macromol. Symp. (2002) 163–173, https://doi.org/10.1002/1521-3900(200201)177:1<163::AID-MASY163>3.0.CO;2-W.

[8] M. Niyaz Khan, Micellar Catalysis, CRC Press, 2006, https://doi.org/10.1201/9781420015843.

[9] M.R. Buchmeiser, Polymeric Materials in Organic Synthesis and Catalysis, Wiley-VCH, 2002, https://doi.org/10.1002/3527601856.

[10] M. Schrinner, F. Polzer, Y. Mei, Y. Lu, B. Haupt, M. Ballauff, A. Göldel, M. Drechsler, J. Preussner, U. Glatzel, Mechanism of the formation of amorphous gold nanoparticles within spherical polyelectrolyte brushes, Macromol. Chem. Phys. 208 (2007) 1542–1547, https://doi.org/10.1002/macp.200700161.

[11] Y. Lu, Y. Mei, M. Schrinner, M. Ballauff, M.W. Möller, J. Breu, in situ formation of Ag nanoparticles in spherical polyacrylic acid brushes by UV irradiation, J. Phys. Chem. 111 (2007) 7676–7681, https://doi.org/10.1021/jp070973m.

[12] R.K. O'reilly, C.J. Hawker, K.L. Wooley, Cross-linked block copolymer micelles: functional nanostructures of great potential and versatility, Chem. Soc. Rev. 35 (2006) 1068–1083, https://doi.org/10.1039/b514858h.

[13] S. Chen, F. Gayet, E. Manoury, A. Joumaa, M. Lansalot, F. D'Agosto, R. Poli, Coordination chemistry inside polymeric nanoreactors: interparticle metal exchange and ionic compound vectorization in phosphine-functionalized amphiphilic polymer latexes, Chem. Eur J. 22 (2016) 6302–6313, https://doi.org/10.1002/chem.201504923.

[14] A. Joumaa, F. Gayet, E.J. Garcia-Suarez, J. Himmelstrup, A. Riisager, R. Poli, E. Manoury, Synthesis of nixantphos core-functionalized amphiphilic nanoreactors and application to rhodium-catalyzed aqueous biphasic 1-octene hydroformylation, Polymers 12 (2020) 1107, https://doi.org/10.3390/POLYM12051107.

[15] H. Wang, C. Fliedel, E. Manoury, R. Poli, Core-crosslinked micelles with A poly-anionic poly(styrene sulfonate)-based outer shell made by RAFT polymerization, Polymer 243 (2022), 102299, https://doi.org/10.1016/j.polymer.2022.124640.

[16] H. Wang, L. Vendrame, C. Fliedel, S. Chen, F. Gayet, F. D'Agosto, M. Lansalot, E. Manoury, R. Poli, Triphenylphosphine-functionalized core-cross-linked micelles and nanogels with a polycationic outer shell: synthesis and application in rhodium-catalyzed biphasic hydrogenations, Chem. Eur. J. 27 (2021) 5205–5214, https://doi.org/10.1002/chem.202004689.

[17] H. Wang, L. Vendrame, C. Fliedel, S. Chen, F. Gayet, E. Manoury, X. Zhang, F. D'agosto, M. Lansalot, R. Poli, Core-cross-linked micelles made by RAFT polymerization with a polycationic outer shell based on poly(1-methyl-4-vinylpyridinium), Macromolecules 53 (2020) 2198–2208, https://doi.org/10.1021/acs.macromol.9b02582.

[18] S.S. Sambou, R. Hromov, I. Ruzhylo, H. Wang, A. Allandrieu, C. Sabatier, Y. Coppel, J.C. Daran, F. Gayet, A. Labande, E. Manoury, R. Poli, Amphiphilic polymeric nanoreactors containing Rh(I)-NHC complexes for the aqueous biphasic hydrogenation of alkenes, Catal. Sci. Technol. 11 (2021) 6811–6824, https://doi.org/10.1039/d1cy00554e.

[19] H. Wang, A.M. Fiore, C. Fliedel, E. Manoury, K. Philippot, M.M. Dell'Anna, P. Mastrorilli, R. Poli, Rhodium nanoparticles inside well-defined unimolecular amphiphilic polymeric nanoreactors: synthesis and biphasic hydrogenation catalysis, Nanoscale Adv. 3 (2021) 2554–2566, https://doi.org/10.1039/d1na00028d.

[20] A.F. Cardozo, C. Julcour, L. Barthe, J.F. Blanco, S. Chen, F. Gayet, E. Manoury, X. Zhang, M. Lansalot, B. Charleux, F. D'Agosto, R. Poli, H. Delmas, Aqueous phase homogeneous catalysis using core-shell nanoreactors: application to rhodium-catalyzed hydroformylation of 1-octene, J. Catal. 324 (2015) 1–8, https://doi.org/10.1016/j.jcat.2015.01.009.

[21] F. D'Agosto, J. Rieger, M. Lansalot, RAFT-mediated polymerization-induced self-assembly, Angew. Chem. 59 (2020) 8368–8392, https://doi.org/10.1002/anie.201911758.

[22] H. Wang, C.J. Abou-Fayssal, C. Fliedel, E. Manoury, R. Poli, Phosphine-functionalized core-crosslinked micelles and nanogels with an anionic poly(styrenesulfonate) shell: synthesis, rhodium(I) coordination and aqueous biphasic hydrogenation catalysis, Polymers 14 (2022) 4937, https://doi.org/10.3390/polym14224937.

[23] E. Lobry, A.F. Cardozo, L. Barthe, J.F. Blanco, H. Delmas, S. Chen, F. Gayet, X. Zhang, M. Lansalot, F. D'Agosto, R. Poli, E. Manoury, C. Julcour, Core phosphine-functionalized amphiphilic nanogels as catalytic nanoreactors for aqueous biphasic hydroformylation, J. Catal. 342 (2016) 164–172, https://doi.org/10.1016/j.jcat.2016.07.023.

[24] S. Chen, A.F. Cardozo, C. Julcour, J.F. Blanco, L. Barthe, F. Gayet, M. Lansalot, F. D'Agosto, H. Delmas, E. Manoury, R. Poli, Amphiphilic core-cross-linked micelles functionalized with bis(4-Methoxyphenyl)Phenylphosphine as catalytic nanoreactors for biphasic hydroformylation, Polymer 72 (2015) 327–335, https://doi.org/10.1016/j.polymer.2015.02.024.

[25] S. Alunni, V. Laureti, L. Ottavi, R. Ruzziconi, Catalysis of the B-elimination of HF from isomeric 2-fluoroethylpyridines and 1-methyl-2-fluoroethylpyridinium salts. Proton-activating factors and methyl-activating factors as A mechanistic test to distinguish between concerted E2 and E1cb irreversible mechanisms, J. Org. Chem. 68 (2003) 718–725, https://doi.org/10.1021/jo020603o.

[26] N. Li, F. Chen, G. Wang, Q. Zeng, Copper-catalyzed C–P cross-coupling of arylmethyl quaternary ammonium salts via C–N bond cleavage, Monatsh. Chem. 151 (2020) 99–106, https://doi.org/10.1007/s00706-019-02535-y.

[27] R. el Abed, F. Aloui, J.P. Genêt, B. ben Hassine, A. Marinetti, Synthesis and resolution of 2-(Diphenylphosphino)Heptahelicene, J. Organomet. Chem. 692 (2007) 1156–1160, https://doi.org/10.1016/j.jorganchem.2006.11.022.

[28] J. Sanmartín, M.R. Bermejo, C.A. Mcauliffe, A. Sousa, M. Fondo, E. Gómez-Fórneas, Synthesis of polymer-supported triphenylphosphine oxide complexes of divalent copper and cobalt. A study on their reactivity with sulfur dioxide, Inorg. Chim. Acta 255 (1997) 269–278, https://doi.org/10.1016/S0020-1693(96)05373-X.

[29] S. Kondo, K. Furukawa, K. Tsuda, Polymeric analogues of triphenylphosphine oxide as stable phase transfer catalysts, J. Polym. Sci. Part A 30 (1992) 1503–1506, https://doi.org/10.1002/POLA.1992.080300731.

[30] C. Li, Y. Wang, D. Sun, H. Li, X. Sun, D. Ma, Z. Ren, S. Yan, Thermally activated delayed fluorescence pendant copolymers with electron- and hole-transporting spacers, ACS Appl. Mater. Interfaces 10 (2018) 5731–5739, https://doi.org/10.1021/acsami.8b00136.

[31] S. Vanicek, M. Podewitz, J. Stubbe, D. Schulze, H. Kopacka, K. Wurst, T. Müller, P. Lippmann, S. Haslinger, H. Schottenberger, K.R. Liedl, I. Ott, B. Sarkar, B. Bildstein, Highly electrophilic, catalytically active and redox-responsive cobaltoceniumyl and ferrocenyl triazolylidene coinage metal complexes, Chem. Eur J. 24 (2018) 3742–3753, https://doi.org/10.1002/chem.201705051.

[32] M. Deimling, M. Kirchhof, B. Schwager, Y. Qawasmi, A. Savin, T. Mühlhäuser, W. Frey, B. Claasen, A. Baro, T. Sottmann, S. Laschat, Asymmetric catalysis in liquid confinement: probing the performance of novel chiral rhodium–diene complexes in microemulsions and conventional solvents, Chem. Eur. J. 25 (2019) 9464–9476, https://doi.org/10.1002/chem.201900947.

[33] J. Nowakowski, S. Nowakowska, G. Srivastava, M. Baljozovic, J. Girovsky, N. Ballav, T.A. Jung, Probing the reactivity of functionalized surfaces by porphyrin metalation, ChemistrySelect 1 (2016) 891–895, https://doi.org/10.1002/slct.201600215.

[34] T. Nishimura, Y. Maeda, T. Hayashi, Asymmetric cyclopropanation of alkenes with dimethyl diazomalonate catalyzed by chiral diene-rhodium complexes, Angew. Chem. 49 (2010) 7324–7327, https://doi.org/10.1002/anie.201003775.

[35] F.H. Hu, L.S. Wang, S.F. Cai, Solubilities of triphenylphosphine oxide in selected solvents, J. Chem. Eng. Data 54 (2009) 1382–1384, https://doi.org/10.1021/je800842z.

[36] P. Das, P. Chutia, D. Kumar Dutta, Efficient carbonylation of methanol catalyzed by rhodium(I) cyclooctadiene complexes with triphenylphosphinechalcogenide ligands, Chem. Lett. 7 (2002) 766–767, https://doi.org/10.1246/cl.2002.766.

[37] R. Bonnaire, D. Diavoust, N. Platzer, Rh NMR studies of organometallic rhodium(I) derivatives, Org. Magn. Reson. 22 (1984) 80–85, https://doi.org/10.1002/mrc.1270220205.

[38] J.L. Castelbou, A. Gual, E. Mercadé, C. Claver, C. Godard, Ligand effect in the Rh-NP catalysed partial hydrogenation of substituted arenes, Catal. Sci. Technol. 3 (2013) 2828–2833, https://doi.org/10.1039/c3cy00388d.

[39] J.L. Castelbou, E. Bresó-Femenia, P. Blondeau, B. Chaudret, S. Castillón, C. Claver, C. Godard, Tuning the selectivity in the hydrogenation of aromatic ketones catalyzed by similar ruthenium and rhodium nanoparticles, ChemCatChem 6 (2014) 3160–3168, https://doi.org/10.1002/cctc.201402524.

[40] A. Serrano-Maldonado, E. Martin, I. Guerrero-Ríos, Pyridine-stabilized rhodium nanoparticles in ionic liquids as selective hydrogenation and transfer hydrogenation catalysts, Eur. J. Inorg. Chem. 2019 (2019) 2861, https://doi.org/10.1002/ejic.201900575.

[41] S.A. Stratton, K.L. Luska, A. Moores, Rhodium nanoparticles stabilized with phosphine functionalized imidazolium ionic liquids as recyclable arene hydrogenation catalysts, Catal. Today 183 (2012) 96–100, https://doi.org/10.1016/j.cattod.2011.09.016.

[42] X. Zhang, A.F. Cardozo, S. Chen, W. Zhang, C. Julcour, M. Lansalot, J.F. Blanco, F. Gayet, H. Delmas, B. Charleux, E. Manoury, F. D'Agosto, R. Poli, Core-shell nanoreactors for efficient aqueous biphasic catalysis, Chem. Eur. J. 20 (2014) 15505–15517, https://doi.org/10.1002/chem.201403819.

[43] M. Guerrero, N.T.T. Chau, S. Noël, A. Denicourt-Nowicki, F. Hapiot, A. Roucoux, E. Monflier, K. Philippot, About the use of rhodium nanoparticles in hydrogenation and hydroformylation reactions, Curr. Org. Chem. 17 (2013) 364–399, https://doi.org/10.2174/1385272811317040006.

[44] F. Martinez-Espinar, P. Blondeau, P. Nolis, B. Chaudret, C. Claver, S. Castillón, C. Godard, NHC-stabilised Rh nanoparticles: surface study and application in the catalytic hydrogenation of aromatic substrates, J. Catal. 354 (2017) 113–127, https://doi.org/10.1016/j.jcat.2017.08.010.

[45] C. Moreno-Marrodan, F. Liguori, E. Mercadé, C. Godard, C. Claver, P. Barbaro, A mild route to solid-supported rhodium nanoparticle catalysts and their application to the selective hydrogenation reaction of substituted arenes, Catal. Sci. Technol. 5 (2015) 3762–3772, https://doi.org/10.1039/c5cy00599j.

[46] H. Ohde, M. Ohde, C.M. Wai, Swelled plastics in supercritical CO2 as media for stabilization of metal nanoparticles and for catalytic hydrogenation, Chem. Commun. 4 (2004) 930–931, https://doi.org/10.1039/b311522d.

[47] M.L. Buil, M.A. Esteruelas, S. Niembro, M. Oliván, L. Orzechowski, C. Pelayo, A. Vallribera, Dehalogenation and hydrogenation of aromatic compounds catalyzed by nanoparticles generated from rhodium bis(Imino)Pyridine complexes, Organometallics 29 (2010) 4375–4383, https://doi.org/10.1021/om1003072.

[48] H. Mao, X. Liao, B. Shi, Amphiphilic tannin-stabilized Rh nanopartciles: a highly active and reusable catalyst in biphasic aqueous-organic system, Catal. Commun. 16 (2011) 210–214, https://doi.org/10.1016/j.catcom.2011.09.038.

[49] J. Schulz, S. Levigne, A. Roucoux, H. Patin, Aqueous rhodium colloidal suspension in reduction of arene derivatives in biphasic system: a significant physico-chemical role of surfactant concentration on catalytic activity, Adv. Synth. Catal. 344 (2002) 266–269.

[50] N. Yan, Y. Yuan, P.J. Dyson, Rhodium nanoparticle catalysts stabilized with a polymer that enhances stability without compromising activity, Chem. Commun. 47 (2011) 2529–2531, https://doi.org/10.1039/c0cc04641h.

[51] J. Schulz, A. Roucoux, H. Patin, Stabilized rhodium(0) nanoparticles: a reusable hydrogenation catalyst for arene derivatives in a biphasic water-liquid system, Chem. Eur. J. 6 (2000) 618–624, https://doi.org/10.1002/(sici)1521-3765(20000218)6:4<618::aid-chem618>3.0.co;2-a.

[52] C. Vollmer, E. Redel, K. Abu-Shandi, R. Thomann, H. Manyar, C. Hardacre, C. Janiak, Microwave irradiation for the facile synthesis of transition-metal nanoparticles (nps) in ionic liquids (ils) from metal-carbonyl precursors and Ru-, Rh-, and Ir-NP/IL dispersions as biphasic liquid-liquid hydrogenation nanocatalysts for cyclohexene, Chem. Eur. J. 16 (2010) 3849–3858, https://doi.org/10.1002/chem.200903214.

[53] E. Baralt, Z.J. Sandra Smith, Z. Jamie Hurwitz, Z.T. István Horváth, R.H. Fish, Homogeneous catalytic hydrogenation. 6. Synthetic and mechanistic aspects of the regioselective reductions of model coal nitrogen, sulfur, and oxygen heteroaromatic compounds using the (η5-Pentamethylcyclopentadienyl)rhodium tris(acetonitrile) dication complex as the catalyst precursor, J. Am. Chem. Soc. 114 (1992) 5187–5196, https://doi.org/10.1021/ja00039a033.

[54] H. Imai, T. Nishiguchi, K. Fukuzumi, Transfer hydrogenation and transfer hydrogenolysis. 13. Hydrogen transfer from cyclic amines to aromatic nitro compounds catalyzed by noble metal salts, J. Org. Chem. 42 (1977) 431–434, https://doi.org/10.1021/jo00433a024.

[55] E. Baráth, Hydrogen transfer reactions of carbonyls, alkynes, and alkenes with noble metals in the presence of alcohols/ethers and amines as hydrogen donors, Catalysts 8 (2018) 671, https://doi.org/10.3390/catal8120671.

[56] M. Studer, C. Wedemeyer-Exl, F. Spindler, H.-U. Blaser, Enantioselective homogeneous hydrogenation of monosubstituted pyridines and furans, Monatsh. Chem. 131 (2000) 1335–1343, https://doi.org/10.1016/S1381-1169(98)00200-3.